

Radar Altimetry as a Robust Tool for Monitoring the Active Lava Lake at Erebus Volcano, Antarctica

N. J. Peters¹, C. Oppenheimer¹, P. Brennan², L. B. Lok², M. Ash³, P. Kyle⁴

¹Department of Geography, University of Cambridge, Downing Place, Cambridge, CB2 3EN, UK

²Department of Electronic & Electrical Engineering, University College London, Torrington Place, London, WC1E 7JE, UK

³PA Consulting Group, Global Innovation and Technology Centre, Back Lane, Melbourn, Herts, SG8 6DP, UK

⁴Department of Earth and Environmental Sciences, New Mexico Institute of Mining and Technology, Socorro, NM 87801, USA

Key Points:

- The level of active lava lakes is a key parameter in their study but surprisingly hard to measure
- Eredar is a new radar system for monitoring surface level of active lava lakes
- At Erebus volcano it collected the longest continuous time series of lake level to date

Corresponding author: Nial Peters, njp39@cam.ac.uk

Abstract

The level of lava within a volcanic conduit reflects the overpressure within a connected magma reservoir. Continuous monitoring of lava level can therefore provide critical insights into volcanic processes, and aid hazard assessment. However, accurate measurements of lava level are not easy to make, partly owing to the often dense fumes that hinder optical techniques. Here, we present the first radar instrument designed for the purpose of monitoring lava level, and report on its successful operation at Erebus volcano, Antarctica. We describe the hardware and data processing steps followed to extract a time series of lava lake level, demonstrating that we can readily resolve ~ 1 m cyclic variations in lake level that have previously been recognised at Erebus volcano. The performance of the radar (continuous, automated data collection in temperatures of around -30°C) indicates the suitability of this approach for sustained automated measurements at Erebus and other volcanoes with lava lakes.

1 Plain Language Summary

Active lava lakes are the exposed top of a volcano’s magmatic plumbing system. Although only found at a handful of volcanoes worldwide, they are important because they allow direct measurements of magmatic processes which at other volcanoes occur underground and out of sight. The surface level of these lakes is an important parameter to monitor because it reflects pressure changes in the underlying magmatic system. However, it is remarkably difficult to measure because their surface is often obscured by the volcanic gases emanating from the lava. We have developed the first radar instrument for monitoring lava lake level, which can effectively “see through” the volcanic gases, providing an accurate measure of lake level regardless of visibility. The radar was deployed at Erebus volcano, Antarctica and successfully recorded the longest continuous measurements of its lava lake’s surface level made to date. The radar was able to clearly resolve the metre-scale variations in lake level that have previously been documented at Erebus. Our study shows that radar is a promising solution for long-duration studies of lava lakes and we are working on refining our design into an operational tool to support volcanological studies and hazard assessment at other volcanoes around the world.

2 Introduction

Open-vent volcanoes maintain magma at or close to the surface, with persistent outputs of heat and gases [Rose *et al.*, 2013]. At the majority of these volcanoes, the interface between the magma and the atmosphere is obscured or only intermittently exposed within a narrow vent. However, a handful of open-vent volcanoes expose magma in plain view from the crater rim, in the form of an active lava lake which may persist for many decades [Tazieff, 1994]. Examples are found at Nyiragongo (D.R. Congo), Erebus (Antarctica) and Erta 'Ale (Ethiopia). Such volcanoes are of particular importance to volcanology as they allow direct observations to be made of magmatic processes that are normally hidden from view. Studies of active lava lakes have revealed many aspects of magma storage, transport, degassing and eruption, highlighting also processes occurring within magma storage zones, conduit and the lake itself [Patrick *et al.*, 2016].

A key parameter in studying lava lakes, is their surface level. This is indicative of pressure variations in the underlying magmatic system [Patrick *et al.*, 2014], and also fluctuates (typically on shorter time scales) in response to shallower processes such as gas accumulation/release from the lake [Orr and Rea, 2012], and flow dynamics in the conduit [Peters *et al.*, 2014a; Jones *et al.*, 2015].

Perhaps somewhat surprisingly, the surface level of active lava lakes is remarkably difficult to measure, especially over the extended time periods required for understanding their behaviour and for operational monitoring. Previous studies [e.g. Patrick *et al.*,

2014] have used thermal camera images, identifying the position of the surface against the back wall of the lake basin (either manually, or using an automated approach) to estimate the surface height. However, the high temperature maintained by the encompassing basin following a rapid draining of the lake makes the margin difficult to identify for an automated system, and manual identification is extremely time consuming. Furthermore, this approach is affected by changes in the basin geometry and cannot detect level changes due to uplift or subsidence of the crater itself. It should also be noted that even at thermal infrared wavelengths, visibility of the lake can be, and particularly at Erebus often is, severely impacted by the volcanic plume. Plume opacity also impedes the use of stereo-imaging systems [Smets *et al.*, 2017] and terrestrial laser scanning (TLS) technologies. TLS is a widely used tool in geoscience [Telling *et al.*, 2017] and although some lava lake studies have been conducted using such devices [e.g., Jones *et al.*, 2015] they are limited to rare time periods of exceptional visibility. TLS instruments are also expensive and delicate making them unsuitable for long-duration deployment at volcanic craters.

Here we demonstrate that radar is an effective solution to lava lake level monitoring. Using a low cost (\sim £3000), custom built radar system, named Eredar, we were able to obtain the longest continuous measurements of lake level at Erebus volcano to date, easily resolving the \sim 1 m variations in level that are typical of its behaviour [Peters *et al.*, 2014a; Jones *et al.*, 2015].

The aims of this article are twofold: (i) To present the design of our radar system and our data processing strategy, which we believe will be of use to researchers undertaking radar system development in other fields, not just volcanology. (ii) To demonstrate the potential of radar for continuous and extended (operational) lava lake surveillance.

3 Erebus Volcano

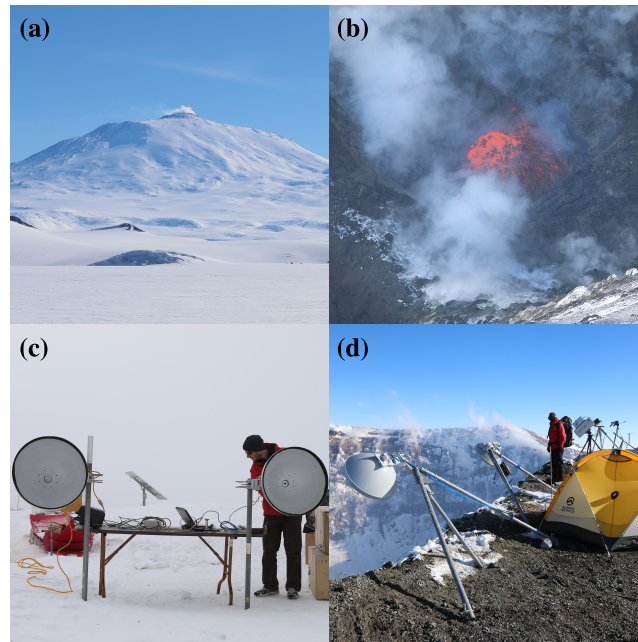
Situated on Ross Island, Antarctica, Erebus is a 3794-m-high active stratovolcano (Fig. 1a). It is the world’s most southerly active volcano, and hosts the only known example of a phonolitic active lava lake (Fig. 1b) [Kelly *et al.*, 2008]. The lake at Erebus has been in place since at least 1972 [Giggenbach *et al.*, 1973], and is characterised by stable convective behaviour punctuated sporadically by Strombolian-type explosions caused by gas slugs entering the lake. Some of these explosions are large enough to partially empty the lake, with ejected material occasionally being thrown clear of the crater [Dibble *et al.*, 2008; Jones *et al.*, 2008]. During periods of quiescence the lake exhibits a remarkable pulsatory behaviour [Oppenheimer *et al.*, 2009], with its surface motion, surface level, gas composition and gas flux all varying on a timescale of 10-15 mins [Peters *et al.*, 2014a]. This behaviour is thought to reflect the flow dynamics of magma in the conduit feeding the lake [Oppenheimer *et al.*, 2009; Peters *et al.*, 2014b], however, a comprehensive explanation has proved elusive and provides, in part, the motivation for the development of the Eredar radar system.

The Erebus lava lake was the subject of a previous study using radar undertaken by Gerst *et al.* [2013]. However, this study focused on analysing the evolution of explosive events in the lake, using a Doppler radar system to measure the expansion rate of large bubbles at the surface. No attempt to monitor the surface level of the lake was made, and the radar system was not considered for long-term deployment.

4 Methods

4.1 Field Deployment

Fieldwork on Erebus is conducted during the Austral Summer, typically between late November and early January. The Eredar radar was deployed on Erebus as part of



110 **Figure 1.** Field deployment of the Eredar radar in December 2016; (a) Erebus volcano, (b) its
 111 active lava lake as it appeared in 2016 (~ 30 m in diameter), (c) Eredar being tested at the field
 112 camp, (d) Eredar installed at the crater rim. The radar electronics are housed in the black case
 113 mounted on the far antenna tripod. The thermal camera and other monitoring instruments can
 114 be seen in the background.

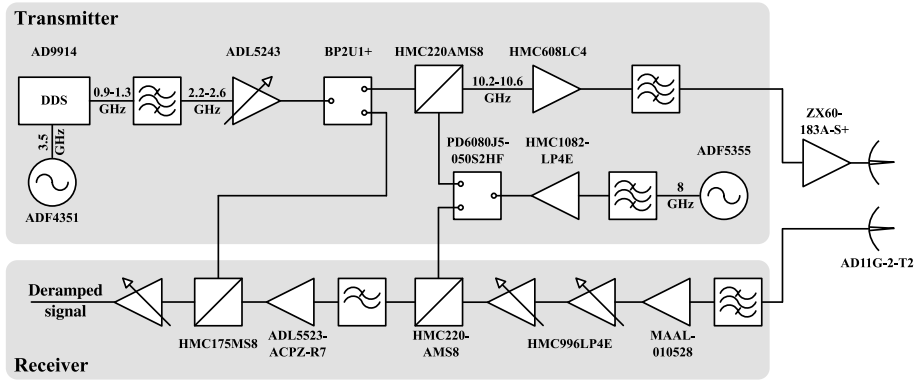
119 the Mount Erebus Volcano Observatory’s (MEVO) 2016 field campaign. Its installation
 120 was hampered by bad weather and it was not in-place until the very end of the campaign,
 121 resulting in a relatively short dataset being obtained.

122 After initial testing at our field camp at around 3450 m elevation (Fig. 1c), The
 123 radar was installed at the so-called “Shackleton’s Cairn” site on the northern side of the
 124 main crater, alongside MEVO’s thermal camera (Fig. 1d) [Peters *et al.*, 2014c]. The an-
 125 tennas were mounted on custom-built heavy duty tripods, which were securely anchored
 126 to the ground. A tent was erected nearby to house the data-acquisition laptop and to
 127 provide shelter for the operator during the setup process. Alignment of the antennas with
 128 the lava lake was achieved by placing an infrared thermometer into their waveguide feeds.
 129 The thermometer had approximately the same field of view (3 degrees) as the antenna
 130 beamwidth (3.6 degrees), and the antennas could then be pointed at the lake by adjust-
 131 ing them until a maximum temperature was recorded. The thermometer was removed
 132 prior to making radar measurements.

133 Following a supervised period of operation lasting ~ 6 hours on 15 December 2016,
 134 the radar was taken down again to avoid damage from an approaching storm. It was then
 135 redeployed on 19 December 2016 and ran, without user intervention, until it had to be
 136 shut-down and removed at the end of the field season (21 hours later). The ambient tem-
 137 perature at the crater rim during this period was approximately -30°C .

138 4.2 Radar Hardware

139 The Eredar instrument is a bespoke, Frequency Modulated Continuous Wave (FMCW)
 140 radar [e.g., Griffiths, 1990; Marshall and Koh, 2008] operating at X-band (10.2-10.6 GHz).



147 **Figure 2.** Simplified block diagram of the Eredar radar system. Some blocks represent an
 148 aggregation of several components and therefore do not have part numbers.

141 Its design is loosely based on two previous geoscience radars constructed by researchers
 142 at University College London, namely the Auto-pRES instrument (UHF, 300 MHz) used
 143 for ice-shelf sounding [Lok *et al.*, 2015] and the Geodar2 system (C-band, 5.3 GHz) used
 144 for avalanche monitoring [Ash *et al.*, 2014]. Due to the requirement of a narrow beamwidth
 145 for lava lake monitoring, the Eredar system operates at much higher frequency than these
 146 previous systems and therefore the details of its design are unique.

149 Figure 2 shows a overview of the Eredar design. An Analog Devices AD9914 Di-
 150 rect Digital Synthesiser (DDS) clocked at 3.5 GHz is used to produce a 900-1300 MHz
 151 linear sweep in frequency. A bandpass filter is then used to select the first super-Nyquist
 152 image [e.g. Ash and Brennan, 2015] of this sweep at 2.6-2.2 GHz. The signal is ampli-
 153 fied, split to provide the deramp signal for the receive chain, and then up-converted us-
 154 ing an 8 GHz source produced by an Analog Devices ADF5355 synthesiser. A bandpass
 155 filter is used to remove unwanted mixing products resulting in a transmitted chirp (lin-
 156 ear frequency sweep) of 10.6-10.2 GHz. A chirp duration of 0.16 seconds was used. To
 157 overcome higher than expected losses in our transmitter chain we included an additional
 158 amplifier between the transmit output and the antenna. This brought our transmitted
 159 power up to ~ 15 dBm. On the receive side, the incoming signal is filtered and ampli-
 160 fied using a chain of three low noise amplifiers, before being down-converted using the
 161 8 GHz signal and subsequently using the deramp signal from the transmitter. The de-
 162 ramped signal is then passed through an active filter stage which performs frequency-
 163 gain control [Stove, 1992, 2004] to compensate for the drop in signal strength with range,
 164 thus maximising the dynamic range available from the system’s analogue to digital con-
 165 verter (ADC). Additionally, the active filter suppresses signals above the Nyquist fre-
 166 quency of the ADC (>40 kHz) and also removes low frequency signals caused by direct
 167 coupling between transmitter and receiver. The filtered, deramped signal is digitised us-
 168 ing a 16 bit ADC clocked at 80 kHz. The ADC clock is precisely aligned with the control
 169 signal to the DDS used to initiate frequency ramping, ensuring inter-chirp coher-
 170 ence in a similar manner to Brennan *et al.* [2014]. Eredar’s on-board microprocessor is
 171 not sufficiently powerful to perform realtime processing on the digitised data. Instead,
 172 it is streamed over Ethernet and recorded on a laptop computer, with all processing be-
 173 ing performed “off-line” at a later date. Ten chirps were averaged for each measurement
 174 and measurements were made at a rate of ~ 0.25 Hz.

175 Both transmit and receive use 66 cm diameter Trango AD11G-2-T2 dish antennas,
 176 with a 3 dB beamwidth of 3.6 degrees and a gain of 36 dBi. Given a range of 315 m and
 177 an incidence angle of 43 degrees (typical viewing geometry of the lake at Erebus; Fig 1d)

178 this gives a beam footprint approximately 27 m in diameter at the surface of the lake.
 179 This is comparable to the lake size itself, which typically varies between 30-50 m in di-
 180 ameter (Fig 1b).

181 The crater rim of Erebus is provided with 230 V AC power from a nearby solar and
 182 wind generation site (see *Peters et al.* [2014c] for details). Due to its requirement of both
 183 positive and negative voltage supplies, the radar uses a centre-tapped transformer and
 184 diode network to step-down and rectify the mains supply producing +7 VDC and -7 VDC.
 185 These supplies are then fed into a bank of linear regulators to produce the various sup-
 186 ply rails required. Switching power supplies were deliberately avoided to keep noise on
 187 the power rails to a minimum. Total power consumption is in the order of 21 W, although
 188 around 50 % of this is dissipated as heat in the linear regulators.

189 The 10.2-10.6 GHz frequency range was selected as a compromise between the cost
 190 of components and the requirement of a narrow beamwidth. For a given antenna size,
 191 beamwidth scales inversely with frequency. However, above 11 GHz there are very few
 192 mass produced components available, resulting in a considerable increase in price.

193 The range resolution of an FMCW radar is given by $\frac{c}{2B}$ where c is the propaga-
 194 tion velocity and B is the bandwidth. High bandwidth radars are more challenging and
 195 costly to construct due to the diminished gap between in-band signals and unwanted spurs,
 196 and the difficulty in wideband matching of components. In addition, for a distributed
 197 target (such as lava lake surface), which will anyway span many range bins, there is lit-
 198 tle need for excessive range resolution since resolving individual reflectors on the lake's
 199 surface is not required. The Eredar system uses a bandwidth of 400 MHz giving a range
 200 resolution of 37.5 cm. This was chosen as a reasonable compromise between range res-
 201 olution and ease and cost of design.

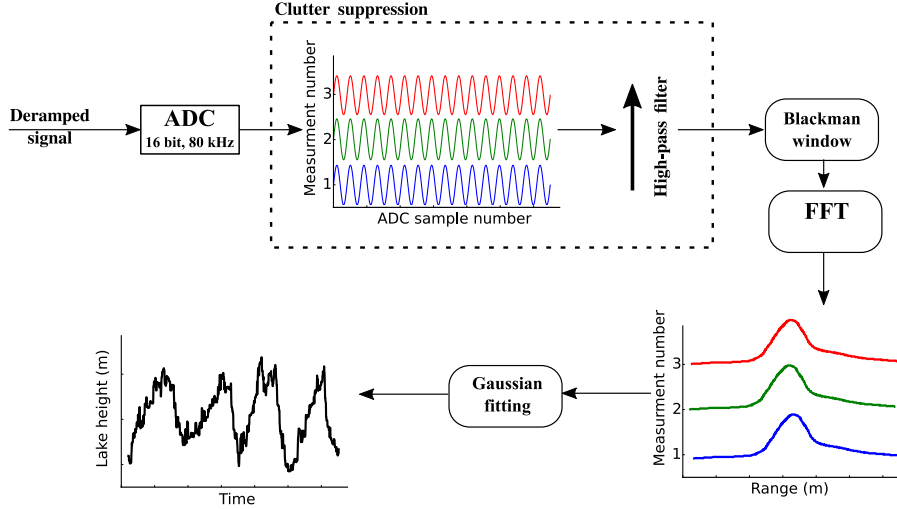
202 The temporal resolution of an FMCW radar is determined fundamentally by the
 203 chirp period used, which in turn is determined by the maximum range required. In the
 204 case of the Eredar system however, the temporal resolution was limited by the data through-
 205 put rate of the microcontroller rather than the chirp period. This limitation was unex-
 206 pected, and will be addressed in future versions of the radar through the use of higher
 207 speed data buses and better optimised software.

208 4.3 Data Processing

209 The data processing steps required to obtain a lake level measurement from the re-
 210 ceiver output are shown in Fig. 3. The data are first conditioned using a clutter suppres-
 211 sion algorithm (described below) to remove stationary targets. They are then windowed
 212 using a Blackman window and Fourier Transformed using an FFT algorithm. The Black-
 213 man window is used to remove edge discontinuities that would otherwise be caused by
 214 the implicit rectangular window imposed by the finite duration of sampling. The win-
 215 dowed data is zero-padded up to a length of 2^{16} prior to applying the FFT. Range is ob-
 216 tained from the frequency (post-FFT) data using the standard FMCW range equation
 217 [e.g. *Griffiths*, 1990] $r = f \cdot \frac{c\tau}{2B}$ where r is range, f is frequency, c is the propagation
 218 velocity, τ is the chirp period and B is the chirp bandwidth. This assumes that objects
 219 are not moving during the chirp period, a reasonable assumption at Erebus where typ-
 220 ical lake surface velocities are in the order of cm s^{-1} [*Peters et al.*, 2014b]. The lake level
 221 is extracted from the range data by applying a Gaussian fit to it, as described below.

229 4.3.1 Clutter Suppression

230 Clutter (unwanted targets within a radar's field of view) is a common problem for
 231 surface viewing radars and many approaches have been developed to suppress it [e.g. *Mar-*
 232 *tone et al.*, 2014; *Hyun et al.*, 2016; *Ash et al.*, 2018]. The crater in which the Erebus
 233 lava lake resides is littered with lava bombs and angular rocks from the crater walls. These



222 **Figure 3.** Block diagram showing the data processing steps required to go from raw receiver
 223 output to lake level measurements. Each chirp is digitised and recorded. The digitised data are
 224 then high-pass filtered across all measurements to remove static clutter. Filtered data are then
 225 Blackman windowed and Fourier Transformed to convert to range. The lake is identified in the
 226 range data by fitting a Gaussian to it. The mean of this Gaussian is used as the slant-range
 227 to the lake. Finally, the slant-ranges may be easily converted to lake level by considering the
 228 viewing geometry.

234 have a much larger radar cross-section compared to the relatively flat surface of the lava
 235 lake and produce strong reflections even when not at boresight. The clutter signal was
 236 found to be so great, that the much weaker lake signal was entirely masked. A common
 237 approach to recovering a moving target signal from a stationary-clutter dominated mea-
 238 surement is to high-pass filter the range-time data to remove stationary targets. Although
 239 this approach was found to work well when recovering point targets (e.g. a person walk-
 240 ing in the radar beam) during testing, it did not work with data collected of the lake.
 241 This was partly due to the low velocity of the lake surface parallel to boresight (on the
 242 order of $1 \times 10^{-3} \text{ m s}^{-1}$), and partly due to the lake being a distributed target. The radar's
 243 oblique view of the lake means that its surface occupies many range bins in the recorded
 244 data. A change in surface level of the lake manifests itself as a rather subtle change in
 245 the distribution of amplitudes across these range bins, and as such is severely muted by
 246 high-pass filtering. Instead, we adopted a similar approach to *Ash et al.* [2018], perform-
 247 ing clutter suppression on the raw radar data prior to conversion to range. Chirps from
 248 a measurement period are stacked coherently in time, and then high-pass filtered before
 249 being Fourier Transformed and converted to range. Such an approach is made possible
 250 by the high degree of coherence between chirps of the Eredar system. We used an in-
 251 finite impulse response (IIR) high-pass elliptic filter with an order of 10 and a cut-off fre-
 252 quency of $3 \times 10^{-2} \text{ Hz}$. Due to the small size of the Erebus lake (relative to the antenna
 253 beamwidth), returns due to antenna sidelobes will be from stationary objects outside of
 254 the lakes surface, and therefore will be effectively removed by the clutter suppression.

255 4.3.2 Lake Level Calculation

256 As noted above, the lake surface spans many range bins and as such manifests it-
 257 self as a broad, smeared-out return rather than a sharp peak in range. Condensing this
 258 into a single value for lake slant-range is somewhat subjective. We trialled three differ-

259 ent approaches to extracting lake level from the radar return data; using the range bin
 260 with the maximum return power, using the lowest range bin above a certain return power
 261 threshold (i.e. the first return from the lakes surface) and fitting a Gaussian function to
 262 the data and using its mean as the slant-range to the lake. The logic of the latter ap-
 263 proach is that to a good approximation, the antenna radiation pattern can be modelled
 264 as a Gaussian. If one assumes an approximately uniform cross-section for all parts of the
 265 lake surface, the shape of the range profile is dominated by the radiation pattern of the
 266 antennas (note that the drop in return power due to increasing range is already accounted
 267 for by the active filter stage in the radar hardware).

268 A distributed target (such as the lakes surface) may be thought of as a large col-
 269 lection of point scatterers. The received signal at the radar is the sum of the contribu-
 270 tions from all the scatterers. Since the lake surface is in constant motion, the phases of
 271 these contributions will be constantly changing, causing differences in return power for
 272 different ranges as the scattering contributions combine in phase or anti-phase. Further-
 273 more, visual inspection of the Erebus lake surface shows that it is far from being a uni-
 274 form collection of scatterers. Numerous cracks in the lakes semi-solid crust exist at any
 275 given instant and these also move with time.

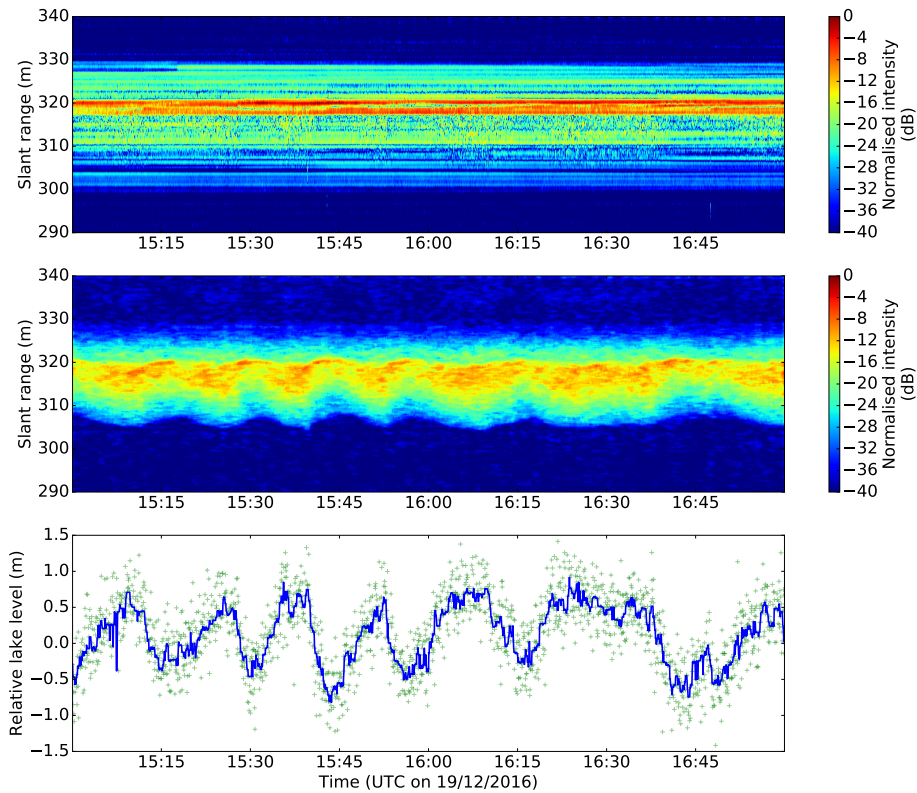
276 Since both the maximum return power and the first return method for identifying
 277 the lake range are based on a single range bin, they are particularly susceptible to the
 278 effects detailed above. It should not be surprising therefore, that although all three tech-
 279 niques give a similar result when time-averaged, the scatter in range is much smaller (ap-
 280 proximately ± 0.5 m) for the Gaussian fit method than for the other methods, which have
 281 a scatter of approximately ± 2 m. For this reason, we found the Gaussian fit method the
 282 most satisfactory for the data presented in this manuscript.

283 The slant-range to the lake was converted to a relative lake level using the follow-
 284 ing equation $L = (\bar{r} - r) \sin \theta$ where L is relative lake level, \bar{r} is mean slant-range (de-
 285 termined from the full time series of measurements), r is slant-range and θ is the graz-
 286 ing angle of the radar beam on the lake surface (measured as 42° using an inclinome-
 287 ter). Thus, a low-stand of the lake (resulting in a higher than average slant-range) gives
 288 a negative value of relative lake level.

289 5 Results and Discussion

290 Figure 4 shows a representative 2 hour window of the data recorded on 19 Decem-
 291 ber 2016. The dominance of static clutter is very evident in the unprocessed data, and
 292 it is somewhat remarkable that a relatively simple clutter-suppression algorithm is so suc-
 293 cessful at removing it and revealing the variations in lake height so clearly. Lake level
 294 is plotted as a relative height about its mean value, showing variations on the order of
 295 ± 0.5 m. This is consistent with the lake level changes measured by *Jones et al.* [2015]
 296 using TLS in 2010. The fluctuations in lake level shown in Fig. 4 exhibit a cyclic behaviour
 297 with a period of ~ 15 min. This is a well-recognised behaviour of the Erebus lake as noted
 298 by numerous previous studies [*Oppenheimer et al.*, 2009; *Peters et al.*, 2014a,b; *Ilnko*
 299 *et al.*, 2015].

300 The lake levels presented in Fig. 4 show a random measurement to measurement
 301 deviation of ± 0.5 m. We attribute this scatter to uncertainties in the Gaussian fitting,
 302 and the rapidly changing specular nature of the lake surface itself. Some measurements
 303 (e.g. at 16:14:20 UTC) show deviations of a few metres from their neighbouring mea-
 304 surements. These are caused by metre-scale bubbles bursting at the lake's surface, form-
 305 ing a strong radar target at a particular range and skewing the Gaussian fit towards that
 306 range. This is confirmed by inspection of coincident thermal imagery collected with an
 307 automated infrared camera system [*Peters et al.*, 2014c].



308 **Figure 4.** Representative 2 hr period of radar data acquired on 19 December 2016 showing
 309 raw slant-range data (top), slant-range data following clutter suppression (middle), lake level
 310 relative to its mean (bottom). Green crosses show the lake level measurements and the blue line
 311 shows the median filtered data (kernel size of 13).

312 6 Conclusions

313 We have presented the Eredar instrument, a new FMCW radar system designed
 314 for monitoring the level of active lava lakes, which was successfully deployed on Erebus
 315 volcano, Antarctica in December 2016. The dataset recorded during this deployment is
 316 the longest continuous measure of lake level at Erebus to date and clearly demonstrates
 317 the potential of radar instruments for prolonged and continuous surveillance of lava lake
 318 level.

319 Future refinement of the system will include reducing power consumption, increas-
 320 ing acquisition rate and incorporating on-board data processing capabilities. The envis-
 321 aged endpoint is a system suitable for long-term operational monitoring in support of
 322 volcanological research and hazard assessment.

323 Acknowledgments

324 This work was supported by the Isaac Newton Trust project "Physical constraints for
 325 the interpretation of open-vent volcanism" and NERC [grant NE/N009312/1]. CO is
 326 additionally supported by the NERC Centre for the Observation and Modelling of Volca-
 327 noes, Earthquakes and Tectonics (COMET). Field support was provided by the NSF un-
 328 der award ANT1142083. NP wishes to thank Aaron Curtis and Tim & Zoe Burton for

329 their help during fieldwork. The radar data presented in this article may be obtained
 330 from <https://doi.org/10.6084/m9.figshare.6480275.v1>.

331 References

- 332 Ash, M., and P. V. Brennan (2015), Transmitter noise considerations in super-
 333 Nyquist FMCW radar design, *Electronics Letters*, *51*(5), 413–415, doi:
 334 10.1049/el.2014.4236.
- 335 Ash, M., M. A. Tanha, P. V. Brennan, A. Köhler, J. N. McElwaine, and C. J. Key-
 336 lock (2014), Improving the sensitivity and phased array response of FMCW radar
 337 for imaging avalanches, in *2014 International Radar Conference*, pp. 1–5, doi:
 338 10.1109/RADAR.2014.7060387.
- 339 Ash, M., M. Ritchie, and K. Chetty (2018), On the Application of Digital Moving
 340 Target Indication Techniques to Short-Range FMCW Radar Data, *IEEE Sensors*
 341 *Journal*, *18*(10), 4167–4175, doi:10.1109/JSEN.2018.2823588.
- 342 Brennan, P. V., L. B. Lok, K. Nicholls, and H. Corr (2014), Phase-sensitive FMCW
 343 radar system for high-precision Antarctic ice shelf profile monitoring, *IET Radar*,
 344 *Sonar & Navigation*, *8*(7), 776–786, doi:10.1049/iet-rsn.2013.0053.
- 345 Dibble, R., P. Kyle, and C. Rowe (2008), Video and seismic observations of Strom-
 346 bolian eruptions at Erebus volcano, Antarctica, *Journal of Volcanology and*
 347 *Geothermal Research*, *177*(3), 619–634, doi:10.1016/j.jvolgeores.2008.07.020.
- 348 Gerst, A., M. Hort, R. C. Aster, J. B. Johnson, and P. R. Kyle (2013), The first
 349 second of volcanic eruptions from the Erebus volcano lava lake, Antarctica - ener-
 350 gies, pressures, seismology, and infrasound, *Journal of Geophysical Research: Solid*
 351 *Earth*, *118*(7), 3318–3340, doi:10.1002/jgrb.50234.
- 352 Giggenbach, W. F., P. R. Kyle, and G. L. Lyon (1973), Present volcanic activity on
 353 Mount Erebus, Ross Island, Antarctica, *Geology*, *1*(3), 135–136.
- 354 Griffiths, H. D. (1990), New ideas in FM radar, *Electronics Communication Engi-*
 355 *neering Journal*, *2*(5), 185–194, doi:10.1049/ecej:19900043.
- 356 Hyun, E., Y.-S. Jin, and J.-H. Lee (2016), A Pedestrian Detection Scheme Using a
 357 Coherent Phase Difference Method Based on 2D Range-Doppler FMCW Radar,
 358 *Sensors*, *16*(1), 124, doi:10.3390/s16010124.
- 359 Ilanko, T., C. Oppenheimer, A. Burgisser, and P. Kyle (2015), Cyclic de-
 360 gassing of Erebus volcano, Antarctica, *Bulletin of Volcanology*, *77*(6), 56, doi:
 361 10.1007/s00445-015-0941-z.
- 362 Jones, K. R., J. B. Johnson, R. Aster, P. R. Kyle, and W. McIntosh (2008), In-
 363 frasonic tracking of large bubble bursts and ash venting at Erebus volcano,
 364 Antarctica, *Journal of Volcanology and Geothermal Research*, *177*(3), 661–672,
 365 doi:10.1016/j.jvolgeores.2008.02.001.
- 366 Jones, L. K., P. R. Kyle, C. Oppenheimer, J. D. Frechette, and M. H. Okal (2015),
 367 Terrestrial laser scanning observations of geomorphic changes and varying lava
 368 lake levels at Erebus volcano, Antarctica, *Journal of Volcanology and Geothermal*
 369 *Research*, *295*, 43–54, doi:10.1016/j.jvolgeores.2015.02.011.
- 370 Kelly, P. J., P. R. Kyle, N. W. Dunbar, and K. W. Sims (2008), Geochemistry and
 371 mineralogy of the phonolite lava lake, Erebus volcano, Antarctica: 1972-2004 and
 372 comparison with older lavas, *Journal of Volcanology and Geothermal Research*,
 373 *177*(3), 589–605, doi:10.1016/j.jvolgeores.2007.11.025.
- 374 Lok, L. B., P. V. Brennan, M. Ash, and K. W. Nicholls (2015), Autonomous phase-
 375 sensitive radio echo sounder for monitoring and imaging antarctic ice shelves,
 376 in *2015 8th International Workshop on Advanced Ground Penetrating Radar*
 377 *(IWAGPR)*, pp. 1–4, doi:10.1109/IWAGPR.2015.7292636.
- 378 Marshall, H.-P., and G. Koh (2008), FMCW radars for snow research, *Cold Regions*
 379 *Science and Technology*, *52*(2), 118–131, doi:10.1016/j.coldregions.2007.04.008.

- 380 Martone, A. F., K. Ranney, and C. Le (2014), Noncoherent Approach for Through-
 381 the-Wall Moving Target Indication, *IEEE Transactions on Aerospace and Elec-*
 382 *tronic Systems*, *50*(1), 193–206, doi:10.1109/TAES.2013.120329.
- 383 Oppenheimer, C., A. S. Lomakina, P. R. Kyle, N. G. Kingsbury, and M. Boichu
 384 (2009), Pulsatory magma supply to a phonolite lava lake, *Earth and Planetary*
 385 *Science Letters*, *284*(3–4), 392–398, doi:10.1016/j.epsl.2009.04.043.
- 386 Orr, T. R., and J. C. Rea (2012), Time-lapse camera observations of gas piston ac-
 387 tivity at Pu’u ’Ō’ō, Kilauea volcano, Hawai’i, *Bulletin of Volcanology*, *74*(10),
 388 2353–2362, doi:10.1007/s00445-012-0667-0.
- 389 Patrick, M. R., T. Orr, L. Antolik, L. Lee, and K. Kamibayashi (2014), Continu-
 390 ous monitoring of Hawaiian volcanoes with thermal cameras, *Journal of Applied*
 391 *Volcanology*, *3*(1), 1, doi:10.1186/2191-5040-3-1.
- 392 Patrick, M. R., T. Orr, D. A. Swanson, and E. Lev (2016), Shallow and deep con-
 393 trols on lava lake surface motion at Kilauea Volcano, *Journal of Volcanology and*
 394 *Geothermal Research*, *328*, 247–261, doi:10.1016/j.jvolgeores.2016.11.010.
- 395 Peters, N., C. Oppenheimer, D. R. Killingsworth, J. Frechette, and P. Kyle (2014a),
 396 Correlation of cycles in Lava Lake motion and degassing at Erebus Volcano,
 397 Antarctica, *Geochemistry, Geophysics, Geosystems*, *15*(8), 3244–3257, doi:
 398 10.1002/2014GC005399.
- 399 Peters, N., C. Oppenheimer, P. Kyle, and N. Kingsbury (2014b), Decadal persistence
 400 of cycles in lava lake motion at Erebus volcano, Antarctica, *Earth and Planetary*
 401 *Science Letters*, *395*, 1–12, doi:10.1016/j.epsl.2014.03.032.
- 402 Peters, N., C. Oppenheimer, and P. Kyle (2014c), Autonomous thermal cam-
 403 era system for monitoring the active lava lake at Erebus volcano, Antarctica,
 404 *Geoscientific Instrumentation, Methods and Data Systems*, *3*(1), 13–20, doi:
 405 10.5194/gi-3-13-2014.
- 406 Rose, W. I., J. L. Palma, H. D. Granados, and N. Varley (2013), Understanding
 407 Open-Vent Volcanism and Related Hazards, Geological Society of America.
- 408 Smets, B., N. d’Oreye, M. Kervyn, and F. Kervyn (2017), Gas piston activ-
 409 ity of the Nyiragongo lava lake: First insights from a Stereographic Time-
 410 Lapse Camera system, *Journal of African Earth Sciences*, *134*, 874–887, doi:
 411 10.1016/j.jafrearsci.2016.04.010.
- 412 Stove, A. G. (1992), Linear FMCW radar techniques, *IEE Proceedings F - Radar*
 413 *and Signal Processing*, *139*(5), 343–350, doi:10.1049/ip-f-2.1992.0048.
- 414 Stove, A. G. (2004), Modern FMCW radar - techniques and applications, in *First*
 415 *European Radar Conference, 2004. EURAD.*, pp. 149–152.
- 416 Tazieff, H. (1994), Permanent lava lakes: observed facts and induced mecha-
 417 nisms, *Journal of Volcanology and Geothermal Research*, *63*(1–2), 3–11, doi:
 418 10.1016/0377-0273(94)90015-9.
- 419 Telling, J., A. Lyda, P. Hartzell, and C. Glennie (2017), Review of Earth science
 420 research using terrestrial laser scanning, *Earth-Science Reviews*, *169*, 35–68, doi:
 421 10.1016/j.earscirev.2017.04.007.